IAC-19-C2.4.4.x50232

Effect of SiC concentration on aero-thermal behavior of ZrB_2-based ceramics in hypersonic environment

Stefano Mungiguerra[a]*, Giuseppe D. Di Martino[a], Anselmo Cecere[a], Raffaele Savino[a], Frédéric Monteverde[b]

[a] *University of Naples "Federico II", Department of Industrial Engineering, Aerospace Division, P.le Tecchio 80, 80125 Napoli, Italy*
[b] *National Research Council of Italy, Institute of Science and Technology for Ceramics, Via Granarolo 64, 48018 Faenza, Italy*
* Corresponding Author, e-mail: stefano.mungiguerra@unina.it

Abstract

This paper presents an extensive experimental campaign over the effect of SiC concentration on the aero-thermal behavior of ultra-high temperature ceramics in the hypersonic atmospheric re-entry environment. Four compositions made of ZrB_2 with different amount of SiC from 5 to 18 vol.% were exposed to the supersonic plasma flow of an arc-heated plasma wind tunnel, at specific total enthalpies up to 20 MJ/kg, measuring their surface temperature by non-intrusive diagnostic equipment, including two-color pyrometers and an infrared thermo-camera. As SiC content increases, maximum steady-state temperature reached on the surface decreased and emissivity value are higher. During some tests, a spontaneous *temperature jump* in the order of 400 K was observed, which only occurred on the front surface of the sample. Surface temperatures over 2800 K were measured after a *temperature jump*. The composition which experienced the *jump* showed an external surface reaction made of only zirconia layer on the front surface, probably appearing upon complete removal of liquid borosilicate glass which forms during exposure to oxygen and is still present on the surface of samples with higher SiC content. The experiments demonstrated that the *temperature jump*, closely related to the overall thermal stability of the material, appears favoured by lower SiC amount, but it can be triggered also in case of larger SiC content (up to at least 15% vol.), as long as the flow total enthalpy and the exposure time are sufficiently high.

Keywords: Ultra-high temperature ceramics; ZrB_2; SiC; arc-jet wind tunnel test; Temperature jump

Nomenclature

H_0	Specific total enthalpy
T	Temperature
t	Time
ε_λ	Spectral emissivity

Acronyms/Abbreviations

BSG	Borosilicate glass
EDM	Electro-discharge machining
HP	Hot Pressing
IR	Infrared
ISTEC	Institute of Science and Technology for Ceramics
NIR	Near Infrared
SEM	Scanning Electron Microscope
SPES	Small Planetary Entry Simulator
TC	Thermo-camera
TPS	Thermal Protection System
UHTC	Ultra-High-Temperature Ceramics
UHTCMC	Ultra-High-Temperature Ceramic Matrix Composite
UNINA	University of Naples "Federico II"

1. Introduction

The extremely demanding aero-thermo-dynamic conditions encountered by hypersonic vehicles during atmospheric re-entry make the design of proper Thermal Protection Systems (TPS) a topic of utmost importance, requiring continuous improvement of materials and technologies [1, 2]. The environment of re-entry includes hypersonic Mach numbers, projected service temperatures above 2000°C or recombination reactions of dissociated gases which can substantially enhance the heat flux on the exposed surface of the spacecraft [3, 4].

Ultra-high temperature ceramics (UHTCs) and, more recently, ultra-high temperature ceramic matrix composites (UHTCMCs), based on transition metals carbides and diborides, are actively studied as candidates for these applications due to their high melting temperature, strength and oxidation resistance at temperatures over 2000°C [5, 6]. Silicon carbide is often added as minor component into UHTC matrices to confer improved performances [7]. The dispersion of SiC in the form of particle, short fiber or whisker, into the main UHTC matrix is frequently used to improve damage tolerance and oxidation resistance thanks to the formation of an oxide protective scale, performing a self-healing function at ultra-high temperatures [8, 9].

For SiC-containing UHTCs and C-SiC based ceramics, a sudden temperature overshoot (*temperature jump*) in the order of 400-500 K occurring at constant flow total enthalpy was observed by several authors, but still several interpretations are proposed, including: transition from passive to active oxidation of silicon carbide [10, 11, 12]; triggering of catalytic recombination of nitrogen atoms due to the presence of gaseous Silicon [13]; formation of cracks promoting oxygen diffusion to inner SiC particles and carbon fibers, resulting in carbon exothermic oxidation and nitridation [12, 14]; surface modifications altering properties of the samples such as emissivity and catalycity [15].

In this framework, University of Naples "Federico II" (UNINA) and the Institute of Science and Technology for Ceramics (ISTEC) are involved in the Horizon 2020 European C^{3}HARME research project, focused on a new class of UHTCMCs for near zero-ablation thermal protection systems [16].

In this work, specific tests were carried out to study the effect of increasing amount of SiC into ZrB_2 UHTC matrices. Lab-scale samples with different SiC amount (5-18% vol.) were tested in the high-enthalpy arc-jet wind tunnel available at UNINA, where atmospheric re-entry conditions are reproduced at maximum flow total enthalpies higher than 20 MJ/kg, supersonic Mach number and temperatures over 2000°C in a gas atmosphere with high concentration of atomic oxygen. Non-intrusive diagnostic tools, including two-color pyrometers and an infrared thermo-camera, were employed to monitor the surface temperature of the samples. The present paper is organized as follows. Section 2 describes the experimental setup used to evaluate the material responses. Section 3 describes the experimental results obtained for four different materials having different SiC content. Then, results are discussed in Section 4, primarily addressing the effect of SiC content on the material behaviour, in terms of oxidation resistance, maximum equilibrium temperature, surface emissivity and the occurrence of the *spontaneous temperature jump*.

2. Material and methods

2.1 Experimental Setup

To characterize materials response to the extreme aero-thermo-chemical environment, lab-scale samples shaped as flat round button were exposed to a high-enthalpy supersonic dissociated air flow, typical of re-entry conditions, using the arc-jet wind tunnel available at the University of Naples "Federico II", named SPES (Small Planetary Entry Simulator, Fig. 1). This is an open circuit, continuous wind tunnel where a nitrogen plasma can be generated by an industrial torch able to operate at powers up to 80 kW and mixed to a secondary cold oxygen flow used to simulate the earth atmospheric composition. A converging-diverging nozzle is employed to expand the hot mixture to a nominal supersonic Mach number equal to 3. A detailed facility description can be found in [17] while an overall view of the test facility is shown in Fig. 1b). The wind tunnel is equipped with several optical accesses allowing real time monitoring of the test by means of infrared and optical diagnostic technique.

Samples are placed at a fixed distance with respect to the nozzle exit by a dedicated thermally protected supporting mechanism, Fig. 1a). The surface temperature of the sample was continuously measured (±1% instrumental accuracy) by digital two-color pyrometers (Infratherm ISQ5 and IGAR6, Impac Electronic GmbH, Germany) at an acquisition rate of 100 Hz. In addition, an infrared (IR) thermo-camera (TC, Pyroview 512N, DIAS Infrared GmbH, Germany) allows for the evaluation of the temperature distribution over the sample surface.

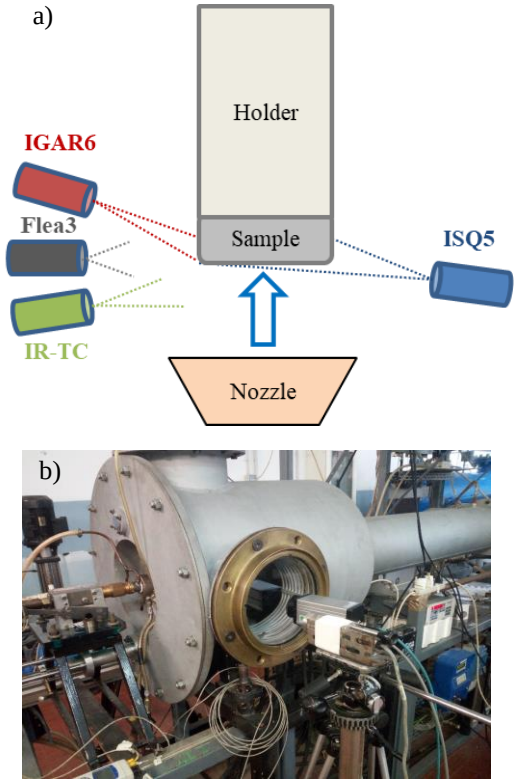

Fig. 1. The experimental setup. a) Optical setup. b) SPES arc-jet wind tunnel available at UNINA.

The ISQ5 pyrometer exploits two overlapping infrared wavelength bands at 0.7–1.15 μm and 0.97–1.15 μm to measure the actual temperature from 1273 K up to 3273 K. The IGAR6 pyrometer operates in the bands 1.5-1.6 μm and 2.0-2.5 μm to return the sample temperature in the range 523-2773 K. The measurement area of the ISQ5 pyrometer is approximately a round spot 3.3 mm in diameter. The thermo-camera is able to

detect temperature in the range 873-3273 K and it operates in the spectral range from 0.8 to 1.1 μm. The procedure employed to set the correct value of spectral emittance, on which the IR-TC measurement is dependent, is reported in [17].

The nominal design of the sample used for the present test campaign is displayed in Fig. 2. The samples were placed at a distance of 1 cm from nozzle exit. High-Definition videos of the tests were recorded by means of a Camera Flea3 1.3 MP Color USB3 Vision with a resolution of 1328x1048 and a frame rate equal to 25 fps.

2.2 Material samples

Samples were manufactured, all based on a ZrB_2-matrix, but with different amount of SiC varying from 5 to 18 vol.%. In the following the different samples will be labelled:

- ZS05: 95% ZrB_2 – 5% SiC
- ZS10: 90% ZrB_2 – 10% SiC
- ZS15: 85% ZrB_2 – 15% SiC
- ZS18: 82% ZrB_2 – 18% SiC

The base compositions ZSxx were prepared by mixing commercial powders of ZrB_2 and SiC in due proportions, and then hot-pressed at about 1900°C applying 30 MPa. From the sintered billets samples in the shape shown in Fig. 2 were obtained via electro-discharge machining (EDM).

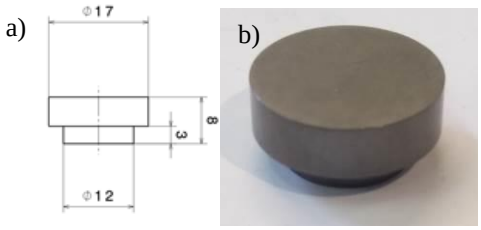

Fig. 2. a) Nominal design main dimension of UHTCMC samples b) A typical sample (ZS15) before test.

2.3 Experimental procedure

Three test sequences were performed. During the first test sequence (test sequence 1), all the samples were exposed to the supersonic plasma flow at stepwise increasing enthalpy steps (see Table 1).

Typically, the test starts with a minimum current of 250 A and it is gradually increased until 600 A. The specific total enthalpy was evaluated through a thermal balance.

After the test, 1.5mm of oxidized material was removed from the top surface and the test repeated (test sequence 2a).

Finally, some samples were subjected to a third sequence (test sequence 2b), without any further surface "refreshing". Further details and the rationale behind the test conditions selection will be given in next sections. Mass before and after each test was measured by means of an electronical balance (±1 mg accuracy).

Table 1. Test conditions

Step	Current [A]	Power [kW]	Specific total enthalpy [MJ/kg]
1	250	12	6
2	300	15	8
3	350	18	10
4	400	21.5	12
5	450	25	14
6	500	29	16
7	550	33	18
8	600	36.5	20

3. Experimental results

3.1 Test sequence 1

During the test sequence 1, all the four samples were subjected to all of the eight enthalpy steps of Table 1. Steps from 1 to 7 had a duration of 30 s, while the last one lasted 120 s. After the most stressful step, the arc power was gradually decreased until facility shutdown. The temperature histories of the four samples during Test sequence 1, measured by ISQ5 pyrometer, are shown in Fig. 3, whereas Fig. 4 shows IR-thermographic and CCD images taken during the tests, together with the visual appearance of the four samples after test. All the samples suffered a relative mass gain around 0.3%.

Some interesting deductions can be argued. First, it is clear that, whereas in the earliest segment of the test the surface temperature of the samples is quite comparable, it tends to deviate for increasing enthalpy steps, until the maximum radiative equilibrium temperature, which appears to be higher for decreasing SiC content.

Worth of mention is the behavior of sample ZS05, which experienced a *spontaneous temperature jump* (recorded by the two-color pyrometer) when surface temperature approached 2150 K, during step 7 (H_0 = 18 MJ/kg). After reaching an almost steady state, the temperature suddenly increased by more than 400 K. The steady state equilibrium temperature would have probably exceeded 2600 K, but the power was increased to the last step before the equilibrium was reached. The final sample temperature was around 2750 K.

Another interesting feature is that, at the maximum enthalpy, the surface temperature oscillates, with higher amplitudes for the samples with increasing SiC content.

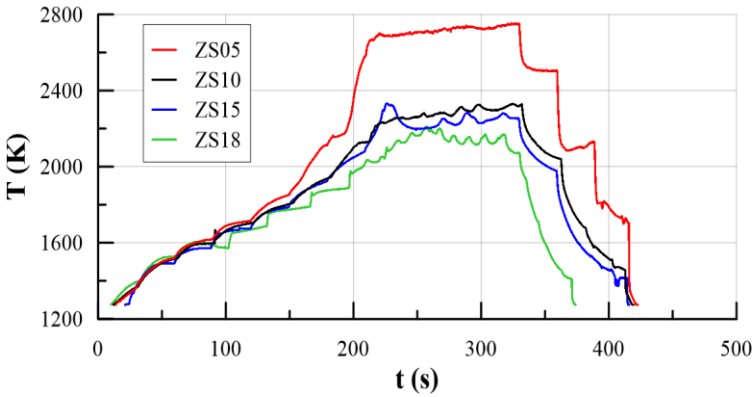

Fig. 3. Temperature histories of the four samples during Test sequence 1, measured by ISQ5 pyrometer

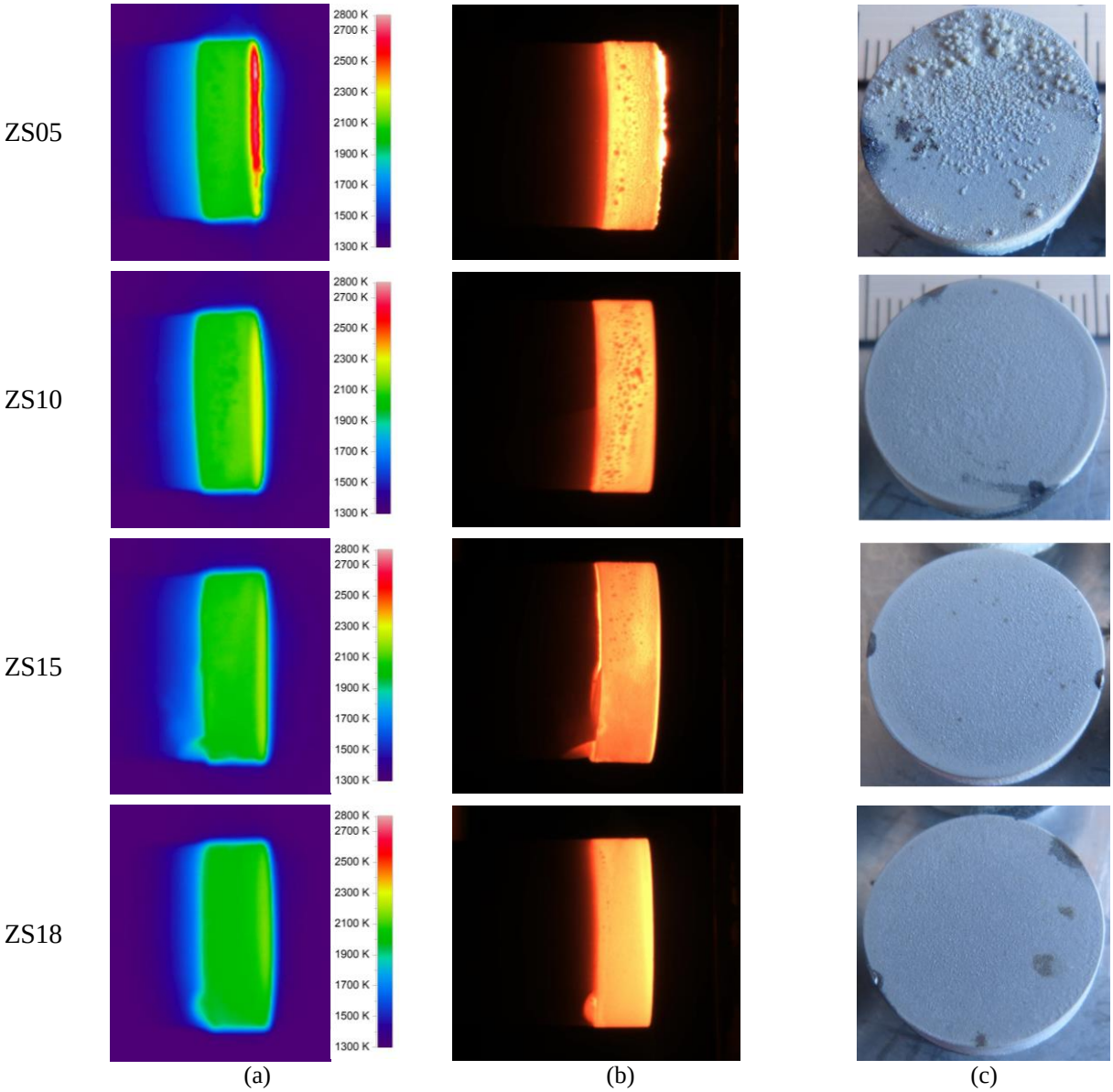

Fig. 4. For the four samples and Test sequence 1 (a) IR thermographic image during last enthalpy step (H_0 = 20 MJ/kg), (b) CCD picture during the cooling phase, (c) appearance of the sample after test

The four samples have a different visual appearance after test, with an evident effect of the increasing SiC content, which affects mostly the resulting roughness of the surface. In particular, sample ZS05, which experienced the *temperature jump*, does not have a compact oxide layer, but its surface shows the formation of irregular protrusions primarily made of zirconia (see Fig. 5). The granular structure on the front surface is highlighted also in the corresponding video snapshot of Fig. 4b, where it appears to be brighter than the rest of the sample during cool down.

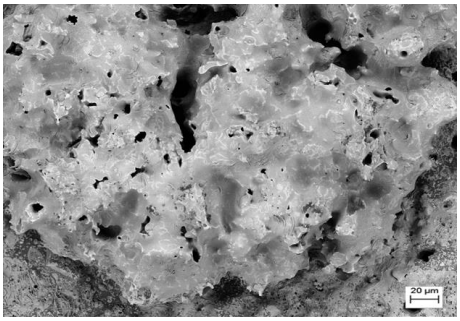

Fig. 5. Surface of ZS05 after test sequence 1 by SEM: an irregular zirconia protrusion is shown

Fig. 6a shows some frames of the video recorded during the test on sample ZS05, taken just before the occurrence of the *temperature jump*. Liquid droplets are wiped away by the surface under the influence of the supersonic plasma flow. Fig. 6b shows that some "flashes" were also observed on the top region of the front surface, during the last enthalpy step, after the occurrence of the *jump*. Despite the brightness saturation, the change in the shape of the front surface, due to the zirconia grains protrusion, is clearly noticeable.

Fig. 7 shows a sequence of IR-TC pictures taken during step 8 of test on ZS15. It is possible to notice, on the bottom part of the side surface, an unsteady evolution of the irradiated power, resulting in a change in the surface color. The same behavior was observed also for the other samples. A similar phenomenon was observed by Monteverde et al. [17], who called it *waves of radiance* and correlated it to the transport of a liquid glassy oxide phase from the front surface along the side of the sample by the shear stresses induced by the supersonic flow.

Fig. 8 shows the spectral emissivity of the four samples versus surface temperature, obtained by matching the measurements of the ISQ5 pyrometer and the IR thermo-camera, in the Near Infrared (NIR) wavelength band. The emissivity tends to increase at the beginning of the tests, up to a maximum value that ranges between 0.8 and 0.9, at temperatures between 1600 and 1700 K, then it decreases for all the samples, assuming higher values for the samples with higher SiC content. After the temperature jump, the spectral emissivity of sample ZS05 increases again up to 0.75 at the maximum temperature of 2750 K.

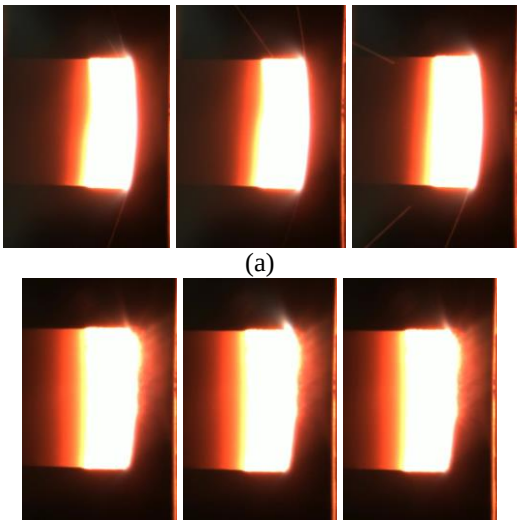

(a) (b)

Fig. 6. Pictures taken (a) few seconds before the *temperature jump* and (b) after the *temperature jump* of sample ZS05 in Test sequence 1.

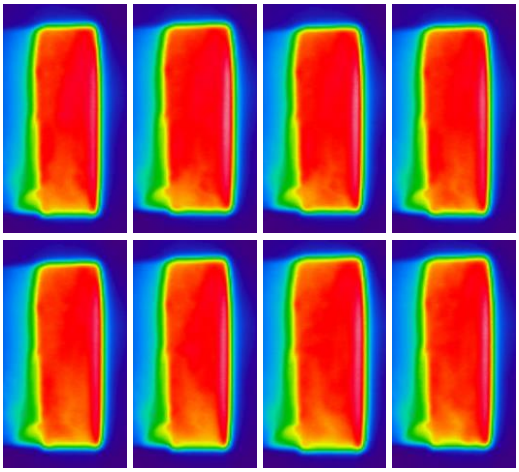

Fig. 7. IR-TC pictures taken during step 8 of test on ZS15, showing *waves of radiance* on the side surface

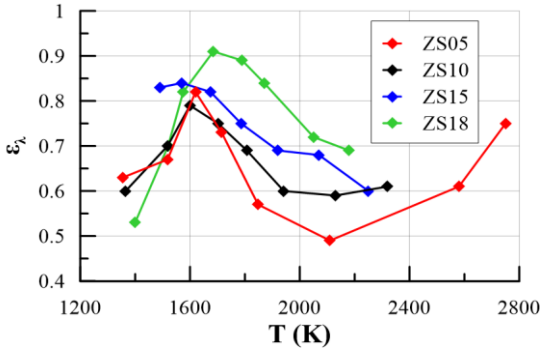

Fig. 8. Samples spectral emissivity versus surface temperature, for test sequence 1

3.2 Test sequence 2a

To better investigate the physics behind the phenomenon of the *spontaneous temperature jump*, additional test sequences were performed. The same buttons were refreshed, by removal of a 1.5 mm thick surface layer, and then exposed to the plasma wind tunnel flow. Fig. 9 shows the appearance of the refreshed ZS05 before the test. The front surface is polished and resembles that of the as-sintered materials (Fig. 2b), whereas the lateral surface is whitened due to the residues of test sequence 1.

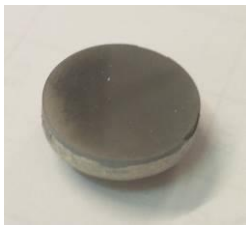

Fig. 9. Appearance of refreshed ZS05 before Test sequence 2a.

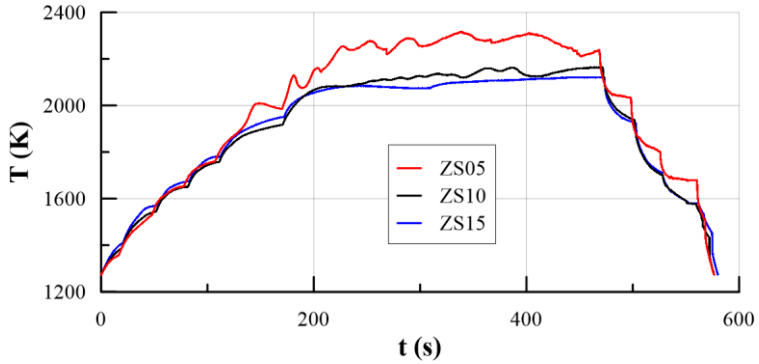

Fig. 10. Temperature histories of the samples during Test sequence 2a, measured by ISQ5 pyrometer

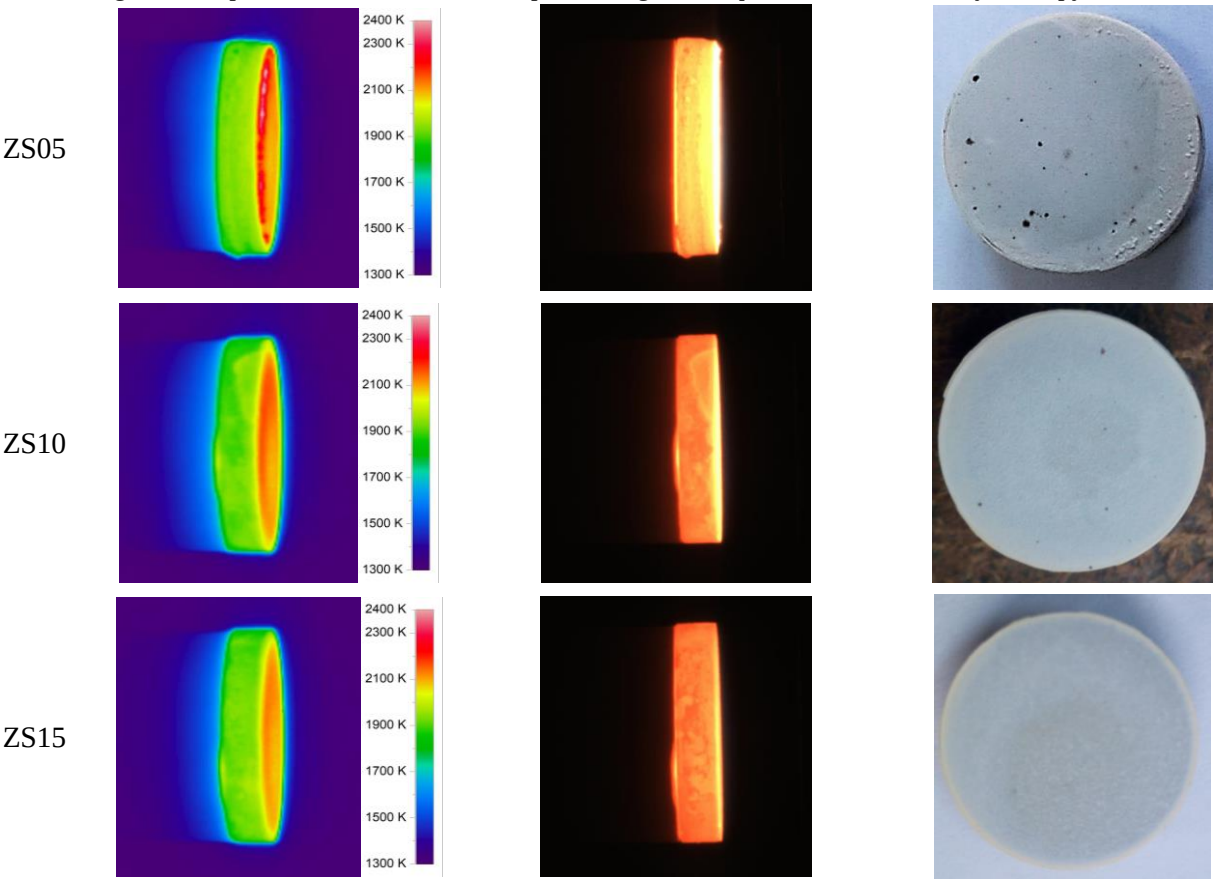

Fig. 11. For the three samples subjected to Test sequence 2a (a) IR thermographic image during last enthalpy step (H_0 = 16 MJ/kg), (b) CCD picture during the last enthalpy step, (c) appearance of the sample after test

In the test sequence 1, ZS05 experienced the *temperature jump*, when the specific total enthalpy was about 18 MJ/kg. The test sequence 2a was intended to assess whether the *jump* could occur also for samples with a higher SiC content, even at lower enthalpy conditions, if the exposure time was sufficiently long. Therefore, in the three tests, the specific total enthalpy corresponding to step 6 (H_0 = 16 MJ/kg) was reached stepwise, so that the sample temperature could exceed, at steady state, at least 2000 K. The duration of the last step was 300 s. For sample ZS15, the power was slightly increased during this step (by 2 kW), to achieve a higher temperature. The corresponding thermal histories, detected by pyrometer ISQ5, are shown in Fig. 10, whereas Fig. 11 shows IR-thermographic and CCD images taken during the tests, together with the visual appearance of the three samples after test.

As can be seen from Fig. 10, no measurable temperature jump was observed in this test sequence 2a. Once again, the steady-state temperature increased for decreasing SiC content, with sample ZS5 reaching the highest equilibrium temperature. In this case, the temperature profile of sample ZS15 did not exhibit any oscillations, whereas they became more evident for decreasing SiC content.

The temperature oscillations find correlations with the oscillation of the surface brightness, as observable in the CCD pictures of Fig. 12. Fig. 12 also highlights the formation of an unstable phase on the front surface, which appears brighter than the side surface and unsteadily changes its shape, with nucleation and bursting of small bubbles.

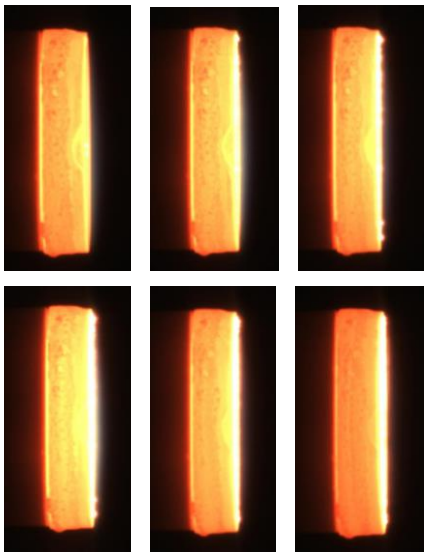

Fig. 12. CCD pictures taken during the last enthalpy step of Test 2a for sample ZS05

Looking at the photographs of Fig. 11c, none of the samples shows protruding zirconia grains, with only some irregular structures on the outer edge of sample ZS05. Relative mass changes were measured in the order of 0.4%. *Waves of radiance* were observed also during this test sequence.

Fig. 13 shows the NIR spectral emissivity for the three samples versus surface temperature. The qualitative trend is the same as in test sequence 1, confirming that the amount of SiC influences ε_λ.

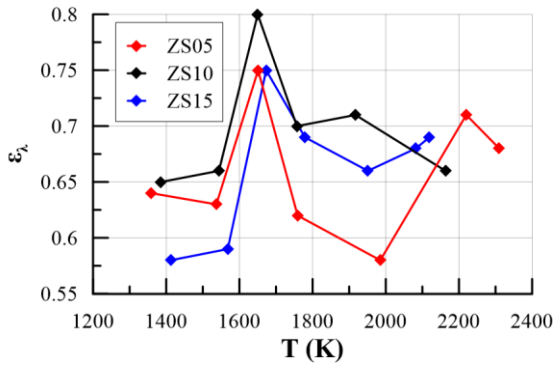

Fig. 13. Samples spectral emissivity ε_λ.versus surface temperature (T), for test sequence 2a

3.3 Test sequence 2b

Because of the absence of *temperature jumps* during test sequence 2a, the two samples ZS10 and ZS15 were subjected to another arc-jet cycle as they came up the test sequence 2a. In this case, the maximum enthalpy (20 MJ/kg) was reached, but with different steps duration. The temperature histories detected by pyrometer ISQ5 are presented in Fig. 14, whereas Fig. 15 shows IR-thermographic and CCD images taken during the tests, together with the visual appearance of the two samples after test.

The thermal histories are different with respect to the previous test sequences. When the temperature of sample ZS10 reached 2200 K (at step 6, H_0 = 16 MJ/kg), it started to rapidly increase, reached a maximum around 2300 K and then started decreasing. After a further enthalpy increase (H_0 = 18 MJ/kg), a similar temperature trend is observable, but still no *jump* was detected. A final increase to the maximum enthalpy level caused the surface temperature to progressively increase until exceeding 2800 K at the end of the step, without even reaching a steady state (after 120 s in those conditions).

Sample ZS15 had a more stable surface temperature history until step 7 (H_0 = 18 MJ/kg), then, when the last enthalpy step was reached, the temperature had a slight increase, then it decreased, reached a plateau around 2320 K and finally started increasing up to 2750 K, with a monotonically increasing trend, without reaching a steady state. The whole duration of the last enthalpy step was 180 s.

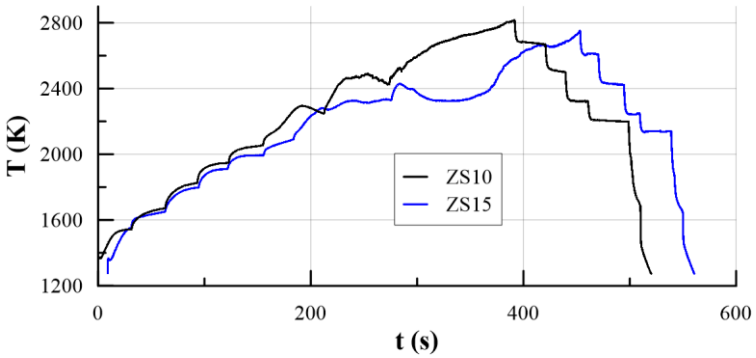

Fig. 14. Temperature histories of the samples during Test sequence 2b, measured by ISQ5 pyrometer

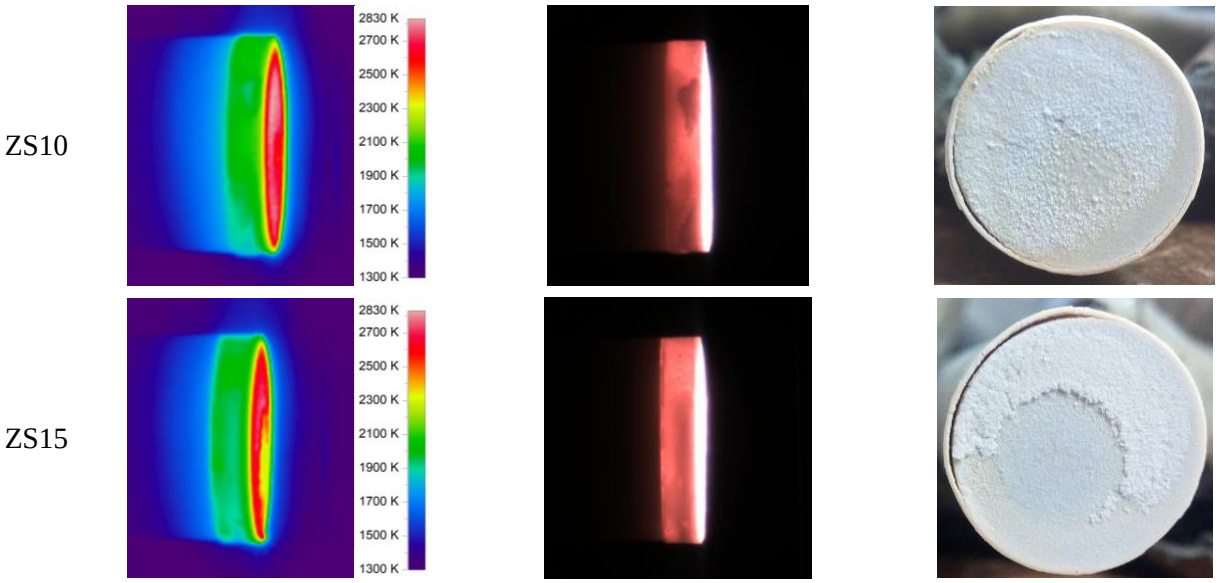

(a) (b) (c)

Fig. 15. For the two samples subjected to Test sequence 2b (a) IR thermographic image during last enthalpy step (H_0 = 20 MJ/kg), (b) CCD picture during the last enthalpy step, (c) appearance of the sample after test

After test, the appearance of both samples front surfaces changed, with the formation of a white irregular surface layer, which covered almost all of the surface of sample ZS10, whereas had a C-shape for sample ZS15. The C-shape can be compared to the shape of the hot region observable in the corresponding IR-TC image (Fig. 15a). Relative mass changes were measured in the order of 0.2%.

Fig. 16 shows some CCD pictures taken during the heating stage of sample ZS10. Also in this case, an unstable brighter zone was observed on the front surface. Liquid droplets were wiped off by the surface (top center picture), while small bubbles appear and disappear during the test. It is also interesting to notice that the brightness of the side surface unsteadily changes while the surface temperature increases. IR thermography confirmed also in this test sequence the presence of the *waves-of-radiance* phenomenon.

Fig. 17 shows the NIR spectral emissivity ε_λ.of the samples during the test sequence 2b, versus their surface temperature. Differently from the first two test campaigns, in this case the ε_λ has an almost monotonic increasing trend, starting for both samples from values above 0.3, reaching a plateau between 2000 and 2350 K, and then increasing to maximum values even over 0.9 when the temperature starts increasing at the end of the test.

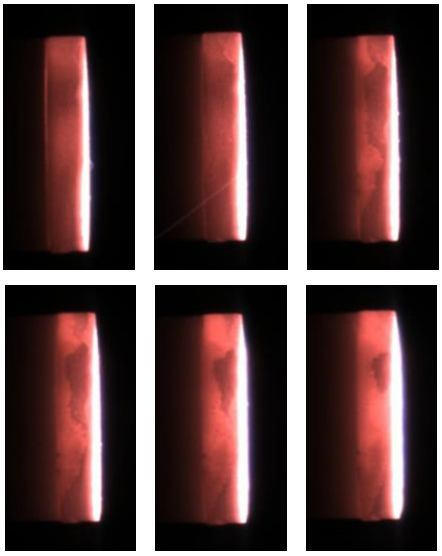

Fig. 16. CCD pictures taken during Test 2b on sample ZS10

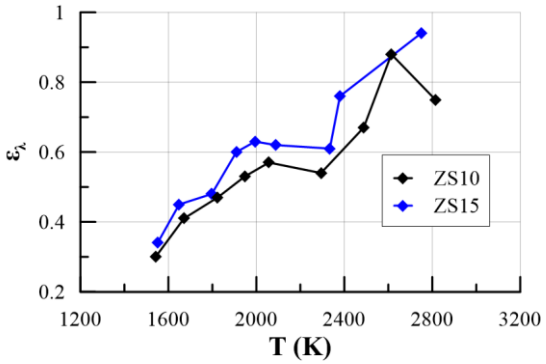

Fig. 17. Spectral emissivity (ε_λ) versus surface temperature (T), for Test sequence 2b

4. Discussion

From the experimental results reported in the previous section, it appears clear that the amount of SiC introduced in ZrB_2-based matrices has measurable effects on its aero-thermal behavior in the high-enthalpy supersonic flow. One of the most evident features is the difference in the maximum equilibrium temperature achieved by the samples, in the same flow conditions. This result was evidently observed both in test sequences 1 and 2a, with increasing equilibrium temperature for decreasing SiC content. This could be also related to the corresponding decrease of surface emissivity, at least in the cases without the *temperature jump*. The observed correlation of SiC concentration with the steady-state temperature is in agreement with what found by Hu et al. [18], who tested ZrB_2-based specimens with a SiC amount ranging from 10 to 30% in a high-enthalpy subsonic wind tunnel. They also found a reduction in the equilibrium temperature for increasing SiC content, associated with an increasing amount of silica glass retained in the sample after ablation. In fact, it is known that higher SiC content promotes a better protection from specimen oxidation, by formation of a Borosilicate glassy phase (BSG) [19]. However, at the temperatures reached during the present test campaigns, boron present in the BGS gets lost through the release of volatile boron oxides [20, 21]. The outer glassy layer, for the samples that did not experience the *jump*, is in our case mainly consisting of silica. Silica melting point is about 2000 K [22], which means that in all the test sequences, at the maximum power conditions, the outer oxide layer was liquid. Indeed, this was confirmed by the CCD pictures shown in section 3, which, as discussed, show the unsteady evolution of this liquid layer, with formation of droplets and bubbles. This liquid glass can be transported downstream, along the side surface of the sample, by the shear stresses induced by the supersonic flow, generating the *waves of radiance* phenomenon described in section 3.1.

A detailed analysis must be carried out to understand the triggers for the phenomenon of the temperature jump. A lower SiC concentration seems to favour an early occurrence of the *jump*: in Test sequence 1, only the sample with the lowest SiC amount experienced the *jump*, whereas in Test sequence 2b, the sample with 10% SiC had a steep rise in temperature in earlier phases of the test with respect to that with 15% SiC, which instead experienced an actual *jump* only when the specific total enthalpy was 20 MJ/kg. Anyway, SiC concentration is probably not the main factor affecting this phenomenon.

All the tests in which a *temperature jump* was observed had some common features:

- An irregular zirconia layer was found on the front surface of the samples after test
- The maximum specific total enthalpy exceeded 18 MJ/kg
- The *temperature jump* takes place only on the front surface of the sample, whereas the rear part of the material keeps a relatively low temperature
- The surface NIR spectral emissivity after the *jump* is higher than before the *jump*

Based on the last bullet, and assuming that the NIR spectral emissivity is representative of the total spherical emissivity, the phenomenon of the *spontaneous temperature jump* cannot be fully attributed to a reduced ability of the material to dissipate the incoming heat flux by radiation. On the other hand, the general trend observed in Test sequences 1 and 2a is in agreement with the total emissivity measurements presented by Scatteia et al. [23], while an increase of ZrO_2 total emittance with temperature was reported by Petrov et al. [24].

On the contrary, it is more likely that the *jump* phenomenon is related to a combination of factors, one of them is a transition in the surface chemistry occurring at ultra-high temperatures. An only zirconia-based scale becomes the outermost thermal barrier of the sample upon removal of the liquid BSG, led by volatilization and mechanical shear. Zirconia is known to have a higher catalytic efficiency with respect to silica [25, 26], which means that the chemical contribution of the heat flux increases after complete silica removal. It has also been demonstrated [27] that for increasing total enthalpies the amount of dissociated oxygen and nitrogen increases, making the catalytic effect more relevant in the determination of the heat fluxes, which could be one of the reasons for the dependence of the *jump* on the flow total enthalpy. Similar features had already been observed on fiber-reinforced UHTCs tested in the same conditions [15], and, based on numerical simulations, the *temperature jump* had been attributed to a twofold mechanism, related to the appearance of the ZrO_2 layer on the front surface: an increase in the chemical contribution to the heat flux, due to an increase of surface catalycity; and a reduction of the thermal conductivity through the exposed oxide layer. The decrease in the thermal conductivity could justify the concentration of the ultra-high-temperatures in the front surface, without propagation to the rear part of the samples.

The understanding of the mechanisms leading to the loss of BSG is key to correctly interpret the *spontaneous temperature jump*. The lower the SiC concentration, the lower the BSG layer thickness and stability, which justifies the earliest occurrence of the *jump* for the samples with limited SiC content. Anyway, observing the results of Test sequence 2a, it is clear that, although all the samples exceeded the melting temperature of BSG, this was insufficient to trigger the *jump* even on the sample ZS05, which on the other hand reached a higher temperature with respect to the *before-jump* condition of Test sequence 1. The presence of zirconia grains nucleation observed on the periphery of that sample after test suggests that the intensity of the shear stresses (which is maximum at the sample edges [28]) could play a not negligible role in determining the onset of the *temperature jump*. Future developments shall include an evaluation of the influence of flow total enthalpy on the shear stresses, to propose a possible interpretation for the dependence of the *temperature jump* onset on the arc-jet conditions.

It should be however pointed out that the results of Test sequence 2b demonstrate that the *jump* can occur also on samples with higher amount of SiC, if the exposure time is sufficiently high.

5. Conclusions

Several experiments were carried out to study the effect of SiC concentration on the aero-thermal behavior of ZrB_2-based Ultra-High-Temperature Ceramic materials in an arc-jet supersonic wind tunnel environment. It was found that, as SiC content increases (from 5 to 18 vol% in the present study), the maximum steady-state temperature reached on sample surface decreases, whereas the Near Infrared spectral emissivity value is higher. Moreover, the experiments were focused on the observation of the *temperature jump*, a sudden and spontaneous increase in temperature in the order of 400-500 K characteristic of UHTCs, which is related to the appearance of a zirconia layer on the front surface of the sample after complete liquid silica oxide removal. The occurrence of the *jump* (which appears only on the front surface of the samples, while the rear part reaches much lower temperatures), is favoured by a low SiC amount, but can happen also for SiC concentrations up to at least 15%. However, it was observed that the flow total enthalpy should be on the order of at least 18 MJ/kg and the exposure time needs to be higher when the SiC amount is higher. Further developments will include more detailed microstructural analyses and Computational Fluid Dynamic simulations for the interpretation of the effects of the flow conditions (including shear stresses) and material properties (surface catalycity, emissivity, thermal conductivity) on the *temperature jump* onset.

Acknowledgements

The C^{3}HARME research project has received funding by the European Union's Horizon2020 research and innovation programme under the Grant Agreement n° 685594.

References

[1] W.G. Fahrenholtz, G.E. Hilmas, Ultra-high temperature ceramics: Materials for extreme environments, Scripta Materialia 129 (2017) 94-99.

[2] R. Savino, S. Mungiguerra, G.D. Di Martino, Testing ultra-high-temperature ceramics for thermal protection and rocket applications, Adv. Appl. Ceram. 117 (sup1) (2018) s9-s18.

[3] E. Wuchina, E. Opila, M. Opeka, W. Fahrenholtz, I. Talmy, UHTCs: Ultra-High Temperature Ceramic materials for extreme environment applications, Electrochem. Soc. Interface 16 (2007) 30-36.

[4] R. Savino, L. Criscuolo, G.D. Di Martino, S. Mungiguerra, Aero-thermo-chemical characterization of ultra-high-temperature ceramics for aerospace applications, J. Eur. Ceram. Soc. 38 (8) (2018) 2937-2953

[5] E. P. Simonenko, et al., Promising Ultra-High-Temperature Ceramic Materials for Aerospace

Applications, Rus. J. Inorg. Chem. 58 (14) (2013) 1669–1693.
[6] L. Silvestroni, H-J. Kleebe, W.G. Fahrenholtz, J. Watts Super-strong materials for temperatures exceeding 2000°C, Sci. Rep. 7 (2017), 40730, doi: 10.1038/srep40730.
[7] T.A. Parthasarathy, D. Petry, M.K. Cinibulk, T. Mathur, M.R. Mark, R. Gruber, Thermal and Oxidation Response of UHTC Leading Edge Samples Exposed to Simulated Hypersonic Flight Conditions, J. Am. Ceram. Soc. 96 (3) (2013) 907-915.
[8] S. Zhou, W. Li, P. Hu, L. Weng, Ablation Behavior of ZrB_2–SiC–ZrO_2 Ceramic Composites by Means of the Oxyacetylene Torch, Corros. Sci. 51 (9) (2009) 2071-2079.
[9] A. Purwar, V. Thiruvenkatam, B. Basu, Experimental and computational analysis of thermo-oxidative-structural stability of ZrB_2–SiC–Ti during arc-jet testing, J. Am. Ceram. Soc. 100 (10) (2017) 4860-4873.
[10] J. Marschall, D. Pejakovic, W.G. Fahrenholtz, G.E. Hilmas, F. Panerai, O. Chazot. Temperature Jump Phenomenon During Plasmatron Testing of ZrB2-SiC Ultrahigh-Temperature Ceramics, J. Thermoph. Heat Transf. 26 (4) (2012) 559-572.
[11] I. Sakraker, C.O. Asma, Experimental investigation of passive/active oxidation behavior of SiC based ceramic thermal protection materials exposed to high enthalpy plasma, J. Eur. Ceram. Soc. 33 (2013) 351-359.
[12] M. Balat-Pichelin, L. Charpentier, F. Panerai, O. Chazot, B. Helber, K. G. Nickel, Passive/active oxidation transition for CMC structural materials designed for the IXV vehicle reentry phase, J. Eur. Ceram. Soc. 35 (2) (2015) 487-502.
[13] H. Hald, Operational limits for reusable space transportation systems due to physical boundaries of C/SiC materials, Aerosp. Sci. Technol. 7 (7) (2003) 551-559.
[14] G. Herdrich, M. Fertig, S. Löhle, S. Pidan, M. Auweter-Kurtz, T. Laux, Oxidation behavior of Silicon carbide-based materials by using new probe techniques, J. Spacecr. Rocket 42 (5) (2015) 817-824.
[15] S. Mungiguerra, G.D. Di Martino, A. Cecere, R. Savino, L. Zoli, L. Silvestroni, D. Sciti, Characterization of carbon-fiber reinforced ultra-high-temperature ceramic matrix composites in arc-jet environment, 69th International Astronautical Congress, Bremen, Germany, 2018, 1 – 5 October.
[16] C3HARME Project Website: https://c3harme.eu/.
[17] F. Monteverde, A. Cecere, R. Savino, Thermo-chemical surface instabilities of SiC-ZrB_2 ceramics in high enthalpy dissociated supersonic air flows, J. Eur. Ceram. Soc. 37 (6) (2017) 2325-2341.
[18] P. Hu, K. Gui, Y. Yang, S. Dong, X. Zhang, Effect of SiC Content on the Ablation and Oxidation Behavior of ZrB_2-Based Ultra High Temperature Ceramic Composites, Mater. 6 (2013) 1730-1744.
[19] L. Zhang, K. Kurokawa, Effect of SiC Addition on Oxidation Behavior of ZrB_2 at 1273 K and 1473 K, Oxid. Met. 85 (2016) 311-320.
[20] K. Shugart, S. Liu, F. Craven, E. Opila, Determination of Retained B2O3 Content in ZrB2-30 vol% SiC Oxide Scales, J. Am. Ceram. Soc. 98 (1) (2015) 287-295.
[21] T.A. Parthasarathy, R.A. Rapp, M. Opeka, M.K. Cinibulk, Modeling Oxidation Kinetics of SiC-Containing Refractory Diborides, J. Am. Ceram. Soc. 95 (1) (2012) 338-349.
[22] W.M. Haynes, CRC Handbook of Chemistry and Physics, 92nd ed., Boca Raton, FL: CRC Press, 2011.
[23] L. Scatteia, D. Alfano, F. Monteverde, J.-L. Sans, M. Balat-Pichelin, Effect of the Machining Method on the Catalycity and Emissivity of ZrB_2 and ZrB_2–HfB_2-Based Ceramic, J. Am. Ceram. Soc. 91(5) (2008) 1461–1468.
[24] V.A. Petrov, A.Y. Vorobyev, A.P. Chernyshev, Thermal radiation and optical properties of cubic zirconia stabilised with yttria up to the temperature of high rate evaporation, High Temp. High Press. 34 (2002) 657-668.
[25] L. Bedra, M. Balat-Pichelin, Comparative modeling study and experimental results of atomic oxygen recombination on silica-based surfaces at high-temperature, Aerosp. Sci. Technol. 9 (2005) 318–328.
[26] M. Balat-Pichelin, M. Passarelli, A. Vesel, Recombination of atomic oxygen on sintered zirconia at high temperature in non-equilibrium air plasma, Mater. Chem. Phys. 123 (2010) 40–46.
[27] S. Mungiguerra, G.D. Di Martino, A. Cecere, R. Savino, L. Zoli, L. Silvestroni, D. Sciti, Arc-jet wind tunnel characterization of ultra-high-temperature ceramic matrix composites, Corros. Sci. 149 (2019) 18-28.
[28] L. Silvestroni, S. Mungiguerra, D. Sciti, G.D. Di Martino, R. Savino, Effect of hypersonic flow chemical composition on the oxidation behavior of a super-strong UHTC, Corros. Sci. 159 (2019) 108125.